A SEARCH FOR MOLECULAR OUTFLOWS ASSOCIATED WITH PECULIAR NEBULOSITIES AND REGIONS OF STAR FORMATION

J.M. Torrelles, L.F. Rodríguez, and J. Cantó

Instituto de Astronomía
Universidad Nacional Autónoma de México

J. Marcaide

Massachusetts Institute of Technology
Cambridge, MA USA

and

A.L. Gyulbudaghian

Byurakan Astrophysical Observatory
Byurakan, Armenian SSR, USSR

RESUMEN

Estudiamos una extensa lista de nebulosidades peculiares y regiones con formación estelar reciente, buscando casos evidentes de emisión de monóxido de carbono con alta velocidad. Asociado a la región de formación estelar GL 2591 hemos encontrado un flujo de gas aparentemente isotrópico. Entre las demás fuentes estudiadas, la nebulosa cometaria GM 24 es interesante puesto que se encuentra localizada en una región molecular muy caliente donde la formación de estrellas masivas tuvo lugar recientemente.

ABSTRACT

We surveyed an extensive list of peculiar nebulosities and regions of star formation searching for conspicuous cases of high-velocity carbon monoxide emission. We detected an apparently isotropic outflow associated with the star-forming region GL 2591. Among the other sources surveyed, the cometary nebula GM 24 is of interest since it is located in a very hot molecular spot where formation of massive stars took place recently.

I. INTRODUCTION

Since the detection of high-velocity carbon monoxide emission in Orion (Zuckerman, Kuiper and Rodríguez-Kuiper 1976; Kwan and Scoville 1976), about 20 other regions showing high-velocity gas motions have been reported. Approximately one half of these flows have a bipolar geometry (Snell, Loren, and Plambeck 1980; Rodríguez, Ho, and Moran 1980; Rodríguez *et al.* 1982; Bally and Lada 1983), that is, their redshifted and blue-shifted emissions arise from spatially separated zones. At the center of the flows there are generally one or more compact objects, such as IR sources, H II regions, or masers, usually believed to indicate the presence of recently formed stars. These gas motions are supposed to be outflows powered by a strong wind from a central young star.

Most of the outflow regions known at present are associated with peculiar nebulosities, such as Herbig-Haro (HH) and Gyulbudaghian Glushkov Denisyuk (GGD), objects, or with regions of recent star formation. On these grounds we searched for conspicuous cases of CO outflow in a list of 103 regions showing either of these two characteristics. The observed sources are the new 22 HH-like objects recently listed by Gyulbudaghian (1982), 73 of the cometary nebulae listed by Parsamian and Petrosian (1979), and 23 other peculiar nebulosities or regions of recent star formation. Some of the observed sources are included in more than one of these lists. In §II we describe the observations, while in §III we discuss the most interesting sources observed. A summary of this work is given in §IV.

II. OBSERVATIONS

The observations of the $J = 1 \rightarrow 0$ rotational transition of CO were made during 1982 March 15-19 with the 11-m radio-telescope of the National Radio Astronomy Observatory[1] at Kitt Peak, Arizona. As receivers we used

147

the 80-120 GHz mixers with orthogonal polarizations and as spectrometers two filter banks in the parallel-parallel configuration ($2 \times 128 \times 100$ kHz and $2 \times 128 \times 500$ kHz). Each polarization was fed into one half of the filter banks and then averaged, resulting in two spectra of 128 channels and velocity resolutions of 0.26 and 1.30 km s^{-1}, respectively. We calibrated the antenna temperatures following Ulich and Haas (1976) and comparing to standard sources. From pointing checks on Jupiter we estimate our rms positional accuracy to be $\sim 15''$. The full width at half maximum of the radio-telescope beam at the observing frequency (115 GHz) is ~ 1.1.

Typical total (reference plus source) integration times were 5 minutes. An observation was made at the position of the source and when the profiles showed evidence of wings, or velocity-displaced components, we did a 3×3 grid at full beam separation centered at the position of the source as given in Tables 1, 2 and 3. These positions usually refer to the centroid of the optical object. In a few cases we added exterior points to the grid trying to include all the region showing line broadening.

Tables 1, 2, and 3 give the observed sources with their main parameters. Table 1 lists regions of star formation and miscellaneous peculiar nebulosities compiled from the literature. Table 2 contains the new list of

nebulosities resembling Herbig-Haro objects found in the Palomar Plates by Gyulbudaghian (1982). Finally, Table 3 lists 73 of the cometary nebulae given by Parsamian and Petrosian (1979).

Given the large number of sources reported in this paper it is possible to investigate some of their statistical properties and compare them with dark clouds where the star formation process, if present, is not so conspicuous. For this purpose we show in Figures 1 and 2 the distribution of sources in antenna temperature and line width for our sample, together with the corresponding distributions for the survey of CO emission in dark clouds by Dickman (1975). There are several interesting differences between the two samples.

Regarding the CO antenna temperatures (Figure 1), our sample does not show the rather narrow distribution of peak antenna temperature about a mean of 6 K shown in the dark cloud sample. Instead we found a continuous (nearly linear) decrease in the number of sources, from very low temperatures ($\lesssim 2$ K) up to about 24 K. Also, our sample contains several sources with rather high antenna temperatures ($\gtrsim 12$ K) which are lacking in the dark cloud sample. The most noticeable in this respect is GM 24 (see § III), which shows a remarkably high antenna temperature of 33 K, much higher than any other source in both samples.

We also notice from this Figure 1 the large number of

TABLE 1

CARBON MONOXIDE OBSERVATIONS
PECULIAR NEBULOSITIES AND REGIONS WITH RECENT STAR FORMATION

| Source | Central Position (1950) | | T_A^* (CO)[b] (K) | V_{LSR}[b] (km s^{-1}) | ΔV[b] (km s^{-1}) |
	α	δ			
LkHα 101 = NGC 1579*	04^{h}26^{m}59^{s}0	35°10'42"	19.8	$-$ 1.0	1.8
CRL 618	04 39 34.0	36 01 15	$\leqslant 1.2$	...	...
HD 44179	06 18 00.0	$-$ 13 43 00	$\leqslant 0.8$	...	...
NGC 2264A	06 38 17.1	09 42 35	16.0	6.5	5.2
NGC 2264B*	06 38 18.3	09 47 17	15.5	8.3	3.1
RE 1[a]	07 48 54.0	$-$ 33 36 26	$\leqslant 1.7$	...	...
RE 2[a]	08 07 40.0	$-$ 35 56 02	7.7	5.7	1.8
RE 3[a]	08 12 24.9	$-$ 36 00 57	7.4	11.5	1.8
HH 55	15 53 18.7	$-$ 37 42 12	11.8	5.2	1.3
RNO 90	16 31 00.0	$-$ 15 41 00	8.3	1.3	1.3
M2 $-$ 9	17 02 53.0	$-$ 10 04 26	$\leqslant 0.5$	...	...
RE 14[a]	17 31 40.0	$-$ 39 11 22	6.3	$-$ 6.0	3.9
RE 15[a]*	17 59 26.3	$-$ 24 17 18	5.7	13.3	5.8
M1 $-$ 91	19 30 51.0	26 48 23	$\leqslant 0.4$	...	...
M1 $-$ 92	19 34 20.0	29 26 07	$\leqslant 0.5$	...	...
GL 2591*	20 27 36.0	40 01 16	11.2	$-$ 5.0	5.5
V1057 Cyg = LkHα 190*	20 57 06.0	44 03 49	4.9	4.8	2.3
CRL 2688 = Egg Nebula	21 00 20.0	36 29 45	1.1	$-$ 36.0	15.6
ELIAS 1 $-$ 12	21 45 27.0	47 18 08	5.5	5.3	4.9

* Mapped sources.
a. From the list of Reipurth (1981).
b. T_A^* (CO) is the peak corrected line antenna temperature, V_{LSR} is the radial velocity with respect to the local standard of rest and ΔV is the full width at half maximum.

TABLE 2

CARBON MONOXIDE OBSERVATIONS
OF NEBULOSITIES RESEMBLING HH OBJECTS[a]

| Source | Central Position (1950) | | T_A^* (CO) (K) | V_{LSR} (km s^{-1}) | ΔV (km s^{-1}) |
	α	δ			
GY 1	00^{h}17^{m}48^{s}0	61°41'00"	4.9	− 29.9	2.6
GY 2 = PP 6 = GM 33	00 33 54.0	63 12 00	7.0	− 18.2	3.9
GY 3	02 55 56.0	17 04 00	2.9	− 5.2	1.9
GY 4 = GL 437	03 03 32.0	58 20 00	14.2	− 40.3	3.9
GY 5	03 13 23.0	59 59 00	5.1	− 14.7	3.1
GY 6	03 33 18.0	37 05 00	2.3	0.6	3.9
GY 7	03 44 31.0	32 50 00	11.2	10.0	2.6
GY 8*	03 48 33.0	38 44 00	3.9	− 2.1	2.1
GY 9 = PP 12 = GM 15	03 57 12.0	36 03 00	⩽ 0.5	...	...
GY 10 = PP 13 = GM 60	04 07 18.0	38 00 00	8.6	− 3.0	2.9
GY 11	04 23 40.0	25 56 00	5.6	7.1	1.9
GY 12*	04 23 58.0	23 53 00	7.1	4.5	1.0
GY 13	04 59 08.0	− 08 57 00	5.1	5.2	1.9
GY 14	05 17 15.0	− 05 56 00	11.8	8.3	1.8
GY 15*	05 29 36.0	12 49 00	10.7	10.3	3.1
GY 16	05 35 34.0	30 34 00	3.5	− 16.9	2.6
GY 17	05 38 41.0	− 08 06 00	9.4	5.8	3.2
GY 18	05 44 00.0	30 34 00	11.7	− 18.2	1.9
GY 19*	06 05 34.0	− 06 25 00	12.6	10.4	1.8
GY 20	17 55 27.0	− 26 07 00	8.0	10.4	4.2
GY 21	21 00 22.0	78 11 00	⩽ 2.1	...	...
GY 22	22 05 06.0	58 48 00	2.7	− 1.3	3.2

* Mapped sources.
a. Gyulbudaghian (1982).

TABLE 3

CARBON MONOXIDE OBSERVATIONS
OF THE PECULIAR NEBULOSITIES LISTED BY PARSAMIAN-PETROSIAN

| Source | Central Position (1950) | | T_A^* (CO) (K) | V_{LSR} (km s^{-1}) | ΔV (km s^{-1}) |
	α	δ			
PP 1	00^{h}04^{m}54^{s}0	65°21'54"	7.6	− 5.2	2.3
PP 2	00 08 42.0	58 32 00	16.0	− 0.8	1.6
PP 3	00 09 06.0	58 32 36	14.1	− 0.5	1.6
PP 4	00 10 00.0	65 15 12	4.4	− 18.2	3.9
PP 5	00 17 30.0	59 02 00	⩽ 0.7	...	...
PP 6 = GY 2 = GM 33	00 33 54.0	63 12 00	7.0	− 18.2	3.9
PP 7	02 53 24.0	60 29 00	14.5	− 39.0	3.9
PP 8 = GM 55	03 22 06.0	30 36 00	5.6	4.4	7.8
PP 9 = GM 13	03 24 48.0	30 02 00	7.6	6.2	3.4
PP 10	03 25 42.0	30 33 36	8.7	6.5	2.9
PP 11 = GM 14	03 50 48.0	38 02 00	7.2	− 2.6	1.6
PP 12 = GY 9 = GM 15	03 57 12.0	36 03 00	⩽ 0.5	...	...
PP 13 = GY 10 = GM 60	04 07 18.0	38 00 00	8.6	− 3.0	2.9
PP 14 = IC 359	04 15 36.0	28 09 00	4.7	7.5	1.3
PP 16	04 18 54.0	28 18 00	⩽ 1.2	...	...
PP 22	04 37 24.0	07 15 30	⩽ 1.0	...	...
PP 23	04 52 48.0	30 29 00	4.4	6.2	1.0
PP 24 = GM 3	04 52 48.0	51 26 00	3.2	3.9	3.9
PP 25 = GM 36	05 12 12.0	09 27 00	⩽ 0.8	...	...
PP 26 = GM 37	05 12 24.0	09 21 00	⩽ 0.8	...	...
PP 27 = GM 38	05 17 06.0	− 05 54 00	11.4	7.8	1.8
PP 28	05 28 06.0	34 09 00	⩽ 1.2	...	...

J.M. TORRELLES *et al.*

TABLE 3 (CONTINUED)

Source	Central Position (1950)		T_A^* (CO) (K)	V_{LSR} (km s^{-1})	ΔV (km s^{-1})
	α	δ			
PP 32	05 33 24.0	− 05 29 48	21.0	11.7	4.4
PP 33	05 33 54.0	− 06 28 00	20.6	8.6	3.1
PP 34 = NGC 1999	05 34 00.0	− 06 44 00	22.0	9.1	3.6
PP 35 = GM 39	05 34 42.0	31 59 00	3.3	− 19.5	3.9
PP 36 = GM 40	05 35 36.0	30 39 00	3.9	− 16.9	3.9
PP 37 = H 13a	05 35 54.0	− 07 03 00	13.3	6.0	3.1
PP 38	05 36 18.0	26 21 00	≤ 1.2	...	...
PP 39	05 36 54.0	− 07 27 00	11.0	6.5	4.4
PP 40 = GM 66	05 37 30.0	35 41 00	10.2	− 18.2	3.9
PP 42	05 39 24.0	− 08 03 00	10.2	5.5	2.9
PP 43 = FU Ori	05 42 38.0	09 03 02	5.5	12.4	1.3
PP 44	05 43 30.0	− 00 13 00	7.1	10.4	2.6
PP 48	05 55 42.0	16 32 00	1.2	7.8	3.9
PP 49	05 59 00.0	16 31 00	2.6	2.6	2.6
PP 50	06 00 00.0	− 09 07 00	≤ 1.0	...	...
PP 51	06 01 06.0	− 09 43 30	7.1	13.5	2.1
PP 52	06 01 18.0	30 31 00	2.7	2.6	2.6
PP 81	15 42 00.0	− 34 08 00	11.1	4.2	2.9
PP 82	16 23 54.0	− 24 39 00	17.3	3.9	2.3
PP 83 = GM 87	16 26 36.0	− 26 40 00	≤ 0.6	...	...
PP 84 = GM 48	16 31 30.0	− 15 41 00	8.0	0.8	1.3
PP 85 = GM 24*	17 13 42.0	− 36 18 00	32.6	− 9.7	6.5
PP 86 = GM 56	18 39 54.0	08 05 00	4.6	16.9	2.6
PP 87 = NGC 6729*	18 58 24.0	− 37 02 00	13.9	+ 6.8	2.6
PP 88	19 26 36.0	09 32 00	≤ 0.5	...	...
PP 89 = NGC 6820 = GM 26	19 40 18.0	22 58 00	15.6	27.3	2.6
PP 90 = GM 27*	20 18 18.0	37 00 00	4.0	2.3	2.1
PP 91	20 19 06.0	41 12 00	6.3	2.3	1.8
PP 92 = V1515 Cyg	20 22 03.0	42 02 40	6.1	6.5	3.2
PP 93 = GM 10	20 22 12.0	35 41 00	8.8	10.1	3.1
PP 94 = GM 11	20 22 30.0	33 51 00	≤ 1.4	...	...
PP 95	20 22 42.0	42 04 18	17.1	5.2	3.9
PP 96 = GM 28	20 23 06.0	35 56 30	≤ 2.4	...	...
PP 97 = PV Cep = Cohen − 1 = GM 29a	20 45 25.0	67 46 44	3.1	2.6	2.6
PP 98	20 57 06.0	43 52 24	4.9	3.9	3.9
PP 99 = LkHα 120 = V 1331 Cyg	20 59 31.0	50 09 45	3.2	0.0	4.5
PP 100	21 02 18.0	67 54 48	8.9	3.6	2.6
PP 101 = GM 12	21 40 42.0	54 41 00	6.3	0.8	2.3
PP 102 = GM 57	21 41 42.0	65 51 00	12.7	− 10.1	2.3
PP 103	22 33 12.0	40 18 12	≤ 0.7	...	...
PP 104 = GM 79	23 03 42.0	59 59 00	13.0	− 50.7	5.2
PP 105	23 35 12.0	48 08 00	3.9	− 7.5	1.3
PP 106	23 56 12.0	66 09 36	2.5	− 6.5	2.3

* Mapped Sources.

a. A detailed mapping of this region by Levreault (1983b) shows a bipolar ouflow with the high velocity lobes displaced symmetrically from our position.

sources in our sample which have very low antenna temperatures (≲ 2 K). This can be due either to very low optical depths of the molecular cloud or to errors in the position for the optical nebulae.

Figure 2 shows the distributions of line widths. In this case we cannot see any sizable or systematic difference between the two samples, except for the Egg Nebula, which shows a line width of ∿ 15 km s^{-1} (Lo and Bechis 1975), at least a factor of two larger than any other source in our sample.

Thirteen of the sources observed showed a spectrum with apparent high velocity components and were mapped for additional information (see Calvet, Cantó, and Rodríguez 1983, for a discussion on real and apparent high-velocity components). These sources are indicated in the tables with an asterisk. However, most of them
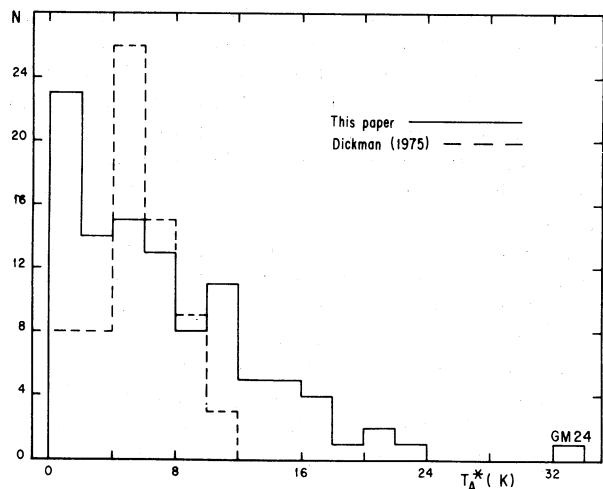
Fig. 1. Distribution of number of clouds as a function of CO antenna temperature for the sample of Dickman (dashed line), and ours (solid line). The bins are 2 K wide.
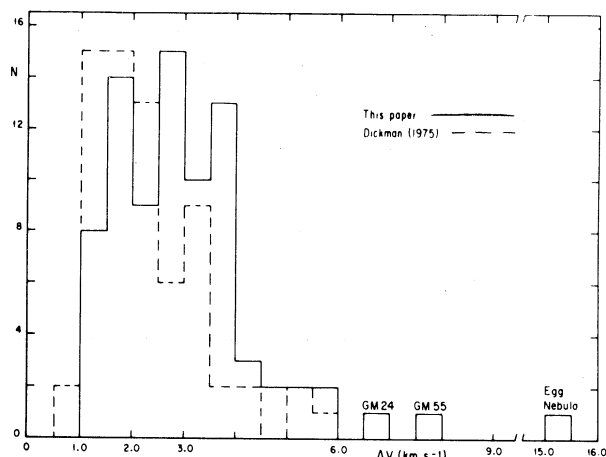

Fig. 2. Distribution of number of clouds as a function of CO line width for the sample of Dickman (dashed line) and ours (solid line). The bins are 0.5 km s^{-1} wide.

showed no significant profile variation when mapped, and thus were rejected as clear cases of localized out-flow. In general, the well-studied outflow sources show drastic variation in their high-velocity emission on the arc minute scale. On the basis of this criterion, only Elias 1-12 and GL 2591 were considered as outflow sources. This low percentage of detected outflows suggests that our sample is not strongly related with promi-nent high-velocity outflows. This may be due to the fact that most of the sources surveyed by us are cometary nebula illuminated by relatively evolved stars that appar-ently do not posses the powerful winds of younger objects. Another possible cause of the low detection rate could be that we surveyed the sources at only one posi-tion and some bipolar outflows are known to have the

high-velocity lobes significantly displaced from its center (for example, L1551, Snell, Loren, and Plambeck 1980; GGD 12-15, Rodríguez et al. 1982; and PV Cep, Lev-reault 1983b). Indeed, PV Cep was observed by us at one position that did not show evidence of high-velocity gas, but a detailed mapping by Levreault (1983b) reveal-ed a bipolar outflow.

The molecular outflow associated with the FU Orionis star Elias 1-12 was detected and studied in detail by Levreault (1983a) and will not be discussed here. In the next section we discuss GL 2591. We also discuss in detail GM 24, a cometary nebula which was found to be associated with a hot and extended molecular region.

III. COMMENTS ON INDIVIDUAL SOURCES

a) GL 2591

This is a luminous IR source ($\gtrsim 3 \times 10^4$ L$_\odot$; Merrill and Soifer 1974) coincident ($\lesssim 1''$) with an H$_2$O maser (Walker et al. 1978; Wynn-Williams et al. 1977). About 7$''$ to the south of the IR/H$_2$O source there is a compact H II region (Wendker and Baars 1974; Wynn-Williams et al. 1977), probably powered by another star.

We mapped at full beam intervals a 5$'$ × 5$'$ region around the central position. The original spectra showed an absorption feature at V$_{LSR}$ = 13.2 km s^{-1} due to CO emission in the reference position, δ (1950) = 20^h 23^m 21$\overset{s}{.}$ 0; δ (1950) = 40° 36$'$35$''$. This absorption was corrected by averaging spectra free of high-velocity emission and subtracting this average spec-trum over the contaminated range. The corrected spec-trum for the central position is shown in Figure 3. It shows wing emission over a velocity range of 32.5 km s^{-1} at a noise level of T$_A$* (rms) $\simeq 0.16$ K. This high-velocity CO emission was detected independ-ently by Bally and Lada (1983). Figure 4 shows a con-
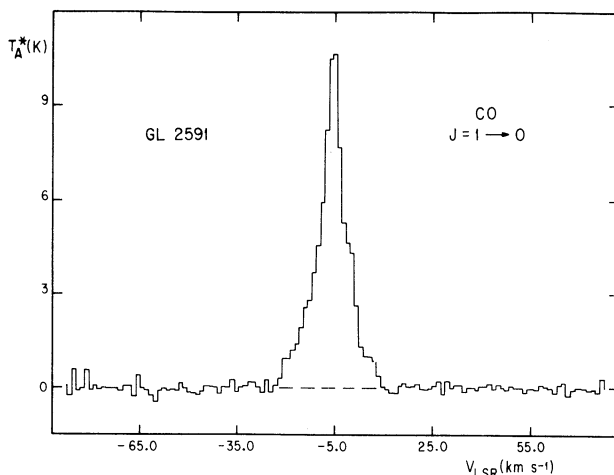

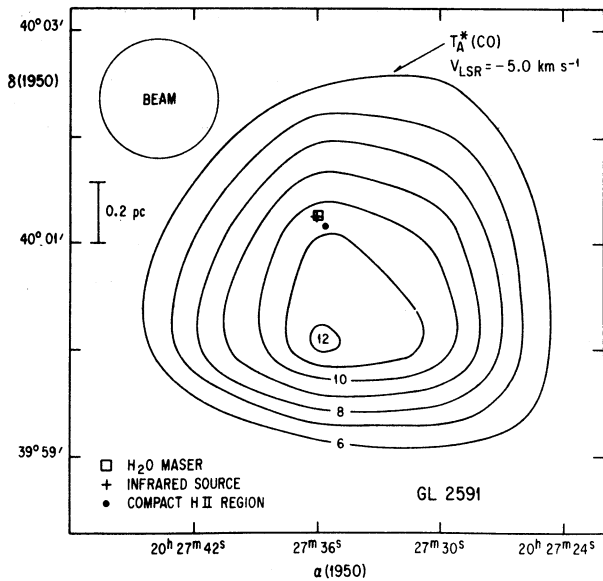Fig. 3. Spectrum of the J = 1 → 0 CO transition for the position of the infrared source GL 2591. The velocity resolution is 1.3 km s^{-1}.

Fig. 4. Contour map of the antenna temperature (in K) at $V_{LSR} = 5.0$ km s^{-1} for GL 2591. Other objects in the region are indicated in the figure.

tour map of the corrected antenna temperature at the radial velocity of the peak T_A^* at the central position, $V_{LSR} = -5.0$ km s^{-1}. The map peaks $\sim 1'$ to the south of the IR source. Figure 5 shows the contours for the integrated blueshifted wing emission for the -22.0 to -11.5 km s^{-1} velocity range. Unfortunately, the redshifted wing emission is contaminated by emission at
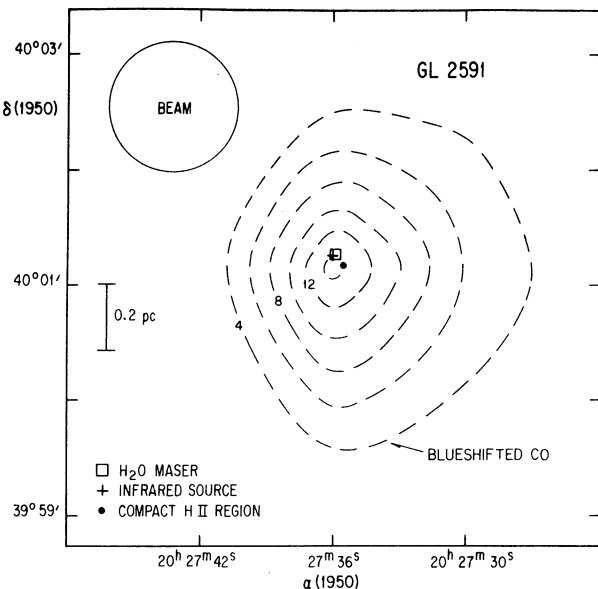

Fig. 5. Contour map of the integrated blueshifted wing emission for the -22.0 to -11.5 km s^{-1} velocity range in GL 2591. Units are in K km s^{-1}.

1.5 km s^{-1} from a line-of-sight cloud and we could not obtain a reliable contour map. However, within considerable uncertainty, it appears that the redshifted gas is roughly spatially coincident with the blueshifted gas, suggesting an apparently isotropic outflow. This suggestion is supported by the spatial coincidence of the centroid of the blueshifted wing emission with the compact objects.

Following Calvet, Cantó, and Rodríguez (1983) we estimated the outflow parameters, which are given in Table 4. The rate of momentum in the outflow, $\dot{M}V$, is $\sim 10^{-4}$ M$_\odot$ yr^{-1} km s^{-1}, a modest value as compared with other molecular outflows. From the results of Rodríguez *et al.* (1982) and Bally and Lada (1983) it seems that, for the known high-velocity molecular outflow sources, $\dot{M}V$ is roughly related to the luminosity of the central source by

$$\left[\frac{\dot{M}V}{M_\odot \ yr^{-1} \ km \ s^{-1}} \right] \sim 10^{-6 \pm 1} \left[\frac{L}{L_\odot} \right]$$

For $L \sim 3 \times 10^4$ L$_\odot$, we would expect $\dot{M}V \sim 3 \times 10^{-2}$ M$_\odot$ yr^{-1} km s^{-1}, a value substantially higher than the observed one. We conclude that GL 2591 is a comparatively weak outflow case for the luminosity of its central sources.

TABLE 4

PARAMETERS OF THE OUTFLOW
ASSOCIATED WITH GL 2591[a]

Parameters	Value
Distance of Associated Cloud[b]	1.5 kpc
Angular Dimensions	2.6 arc min
Physical Dimension	1.1 pc
Mass	1.1 M$_\odot$
Mass Rate	9×10^{-6} M$_\odot$ yr^{-1}
Mass Timescale	1×10^5 yr
Momentum	10.1 M$_\odot$ km s^{-1}
Momentum Rate	1×10^{-4} M$_\odot$ yr^{-1} km s^{-1}
Momentum Timescale	1×10^5 yr
Kinetic Energy	54 M$_\odot$ km^2 s^{-2}
Kinetic Energy Rate	5×10^{-4} M$_\odot$ yr^{-1} km^2 s^{-2}
Kinetic Energy Timescale	1×10^5 yr

a. The definition of the derived mass, momentum and kinetic energy rates and timescales is as given in Calvet, Cantó, and Rodríguez (1983).

b. Data taken from Wendker and Baars (1974).

b) *GM 24*

While all other sources detected by us show $T_A^* \lesssim 20$ K (Figure 1). The molecular cloud associated with GM 24 is considerably hotter, reaching a peak of $T_A^* \simeq 33$ K (Figure 6) at the position of the cometary nebula
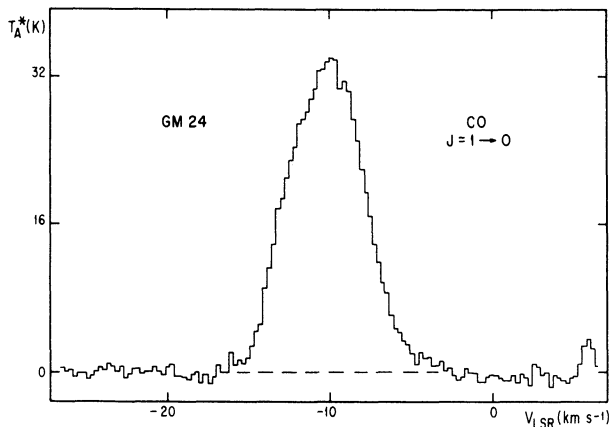
Fig. 6. Spectrum of the $J = 1 \rightarrow 0$ CO transition for the central position of the cometary nebula GM 24. The velocity resolution is 0.26 km s^{-1}.

(Figure 7, Plate). Similar or higher corrected antenna temperatures have only been observed in a few regions of star formation (Wynn-Williams 1982). The high observed T_A^* value indicates the presence of O stars, since very luminous objects are needed to heat the CO (via collisions with hot dust) to the observed temperatures. We can obtain a very crude estimate for the luminosity of the central objects as follows.

From Figure 7 we find that $T_A^* \gtrsim 30$ K for a region of angular radius of $\sim 1'$. Adopting the kinematic distance of 2.0 kpc, this angular size corresponds to a radius of 0.6 pc. Let us consider a range for the molecular hydrogen density from 10^2 to 10^5 cm^{-3}. With this range of particle densities and the heating and cooling formulation of Goldsmith and Langer (1978) we require a dust temperature from 1400 K for 10^2 cm^{-3} to 36 K for 10^5 cm^{-3}, in order to maintain the gas at 30 K. To keep the

dust temperature at 36 K at a distance of 0.6 pc of the central star(s) a luminosity of $\sim 10^5$ L$_\odot$ is required (Loren and Wootten 1978). This luminosity corresponds approximately to that of a O7 ZAMS star (Panagia 1973). Adoption of lower molecular hydrogen densities will make the required star luminosity much higher ($\gtrsim 10^8$ L$_\odot$ for n(H$_2$) $< 10^4$ cm^{-3}), and thus high densities are required.

There is further evidence from other wavelengths of the presence of obscured, and yet undetected, massive stars associated with this cometary nebula. Table 5 gives a list of other radio, far-infrared, and optical sources that probably are associated with GM 24. There are no visible O stars in the zone (Cruz-González et al. 1974). From the broad band far-infrared flux of Emerson, Jennings, and Moorwood (1973) we derive a lower limit for the luminosity of the region of 10^5 L$_\odot$, similar to that derived above for n(H$_2$) $\sim 10^5$ cm^{-3}. Furthermore, Altenhoff et al. (1970) report an extended radio source with a flux of ~ 10 Jy in the centimeter range. Assuming the source to be an optically thin H II region with an electron temperature of 10^4 K, an ionizing rate of $\sim 4 \times 10^{48}$ UV photons s^{-1} is required (Schraml and Mezger 1969) to keep it ionized. Again, this ionizing rate could be provided by an O7 ZAMS star (Panagia 1973). In summary, we may conclude that the molecular cloud to which GM 24 is associated contains at least one massive early-type star.

There are two other optical nebulosities in addition to GM 24. Overlapping the region there is the extended and tenuous Hα emission region RCW 126 (Rodgers, Campbell, and Whiteoak 1960). About $1'$ south of GM 24 there is a bright, elongated ($1' \times 0.5'$) nebula (Figure 7). The relation between these nebulae and the radio and far-infrared sources is not clear at present.

The CO hot spot shows a velocity gradient of ~ 1 km s^{-1} from SE to NW. The FWHM of the CO line

TABLE 5

SOURCES ASSOCIATED WITH GM 24

Source	Central Position (1950)		Angular Extent (arc min)	Reference
	α	δ		
Cometary Nebula GM 24	$17^h13^m42^s.0 \pm 2^s.5$	$-36°18'.0 \pm 0'.5$	0.4	Parsamian and Petrosian (1979)
Far-Infrared Source (HFE 22)	17 13 06 ± 30	-36 20. ± 6	≤ 12	Hoffman et al. (1971)
Far-Infrared Source (UCL 15)	17 14 00 ± 20	-36 17. ± 3	≤ 3.5	Emerson et al. (1973)
Hα Emission Region (RCW 126)	17 13 30 ± 20	-36 18. ± 3	$\sim 16 \times 4$	Rodgers et al. (1960)
Radio Continuum Source (RCW 126)	17 13 48 ± 06	-36 12.1 ± 1	$\sim 15 \times 8$	Altenhoff et al. (1970)
CO Hot Spot	17 13 37.0 ± 1.3	-36 18.0 ± 0.25	$\sim 2 \times 1$[a]	this paper

a. For $T_A^* \geq 30$ K.

IV. CONCLUSIONS

We surveyed an extensive list of peculiar nebulosities and regions of star formation searching for conspicuous cases of high-velocity CO emission. Only Elias 1-12 and GL 2591 showed clear evidence of molecular outflows. Elias 1-12 has been studied in detail by Levreault (1983*a*). GL 2591 is associated with an apparently isotropic outflow of low momentum rate for the luminosity of its central source. This low percentage of detected outflows suggest that our sample is not strongly related with prominent high-velocity outflows because most of the sources surveyed by us are cometary nebulae illuminated by relatively evolved stars that apparently do not possess the powerful winds of younger objects.

The cometary nebula GM 24 is associated with a hot CO spot. From the available data we conclude that this molecular cloud contains at least one obscured O star. This region of recent star formation requires further study.

REFERENCES

Altenhoff, W.J., Downes, D., Goad, L., Maxwell, A., and Rinehart, R. 1970, *Astr. and Ap. Suppl.,* 1, 319.
Bally, J. and Lada, C.J. 1983, *Ap. J.,* 265, 824.
Calvet, N., Cantó, J., and Rodríguez, L.F. 1983, *Ap. J.,* 268, 739.
Cruz-González, C., Recillas-Cruz, E., Costero, R., Peimbert, M., and Torres-Peimbert, S. 1974, *Rev. Mexicana Astron. Astrof.,* 1, 211.
Dickman, R.L. 1975, *Ap. J.,* 202, 50.
Emerson, J.P., Jennings, R.E., and Moorwood, A.F.M. 1973, *Ap. J.,* 184, 401.
Goldsmith, P.F. and Langer, W.D. 1978, *Ap. J.,* 222, 881.
Gyulbudaghian, A.L. 1982, *Pis'ma Astron. Zh.,* 8, 232.
Hoffmann, W.F., Frederick, C.L., and Emery, R.J. 1971, *Ap. J., (Letters),* 170, L89.
Kwan, J. and Scoville, N. 1976, *Ap. J. (letters)* 210, L39.
Levreault, R.M. 1983*a*, *Ap. J.,* 265, 855.
Levreault, R.M. 1983*b*, preprint.
Lo, K.Y. and Bechis, K.P. 1976, *Ap. J. (Letters),* 205, L21.
Loren, R.B. and Wootten, A.H. 1978, *Ap. J. (Letters),* 225, L81.
Merrill, M. and Soifer, B.T. 1974, *Ap. J. (Letters),* 189, L27.
Panagia, N. 1973, *A.J.,* 78, 929.
Parsamian, E.S. and Petrosian, V.M. 1979, *Soobshenia Biurakanskoi Observatori, Akad Nauk Armianskoi S.S.R., No. 51.*
Reipurth, B. 1981, *Astr. and Ap. Suppl.,* 44, 379.
Rodgers, A.W., Campbell, C.T., and Whiteoak, J.B. 1960, *M.N.R.A.S.,* 121, 103.
Rodríguez, L.F., Carral, P., Ho, P.T.P., and Moran, J.M. 1982, *Ap. J.,* 260, 635.
Rodríguez, L.F., Ho, P.T.P., and Moran, J.M. 1980, *Ap. J. (Letters),* 240, L149.
Schraml, J. and Mezger, P.G. 1969, *Ap. J.* 156, 269.
Snell, R.L., Loren, R.B., and Plambeck, R.L. 1980, *Ap. J. (Letters)* 239, L17.
Ulich, B.L. and Haas, R.W. 1976, *Ap. J. Suppl.,* 30, 247.
Walker, R.C. *et al.* 1978, *Ap. J.,* 226, 95.
Wendker, H.J. and Baars, J.W.M. 1974, *Astr. and Ap.,* 33, 157.
Wynn-Williams, C.G. *et al.* 1977, *Ap. J. (Letters),* 211, L89.
Wynn-Williams, C.G. 1982, *Ann. Rev. Astr. and Ap.,* 20, 587.
Zuckerman, B., Kuiper, T.B.H., and Rodríguez-Kuiper, E.N. 1976, *Ap. J. (Letters),* 209, L137.

Jorge Cantó, Luis F. Rodríguez, and José M. Torrelles: Instituto de Astronomía, UNAM, Apartado Postal 70-264, 04510 México, D.F., México.
Jon Marcaide: Massachusetts Institute of Technology, Cambridge, MA 90024, USA.
Armen L. Gyulbudaghian: Byurakan Astrophysical Observatory, Byurakan, Armenian SSR, USSR.
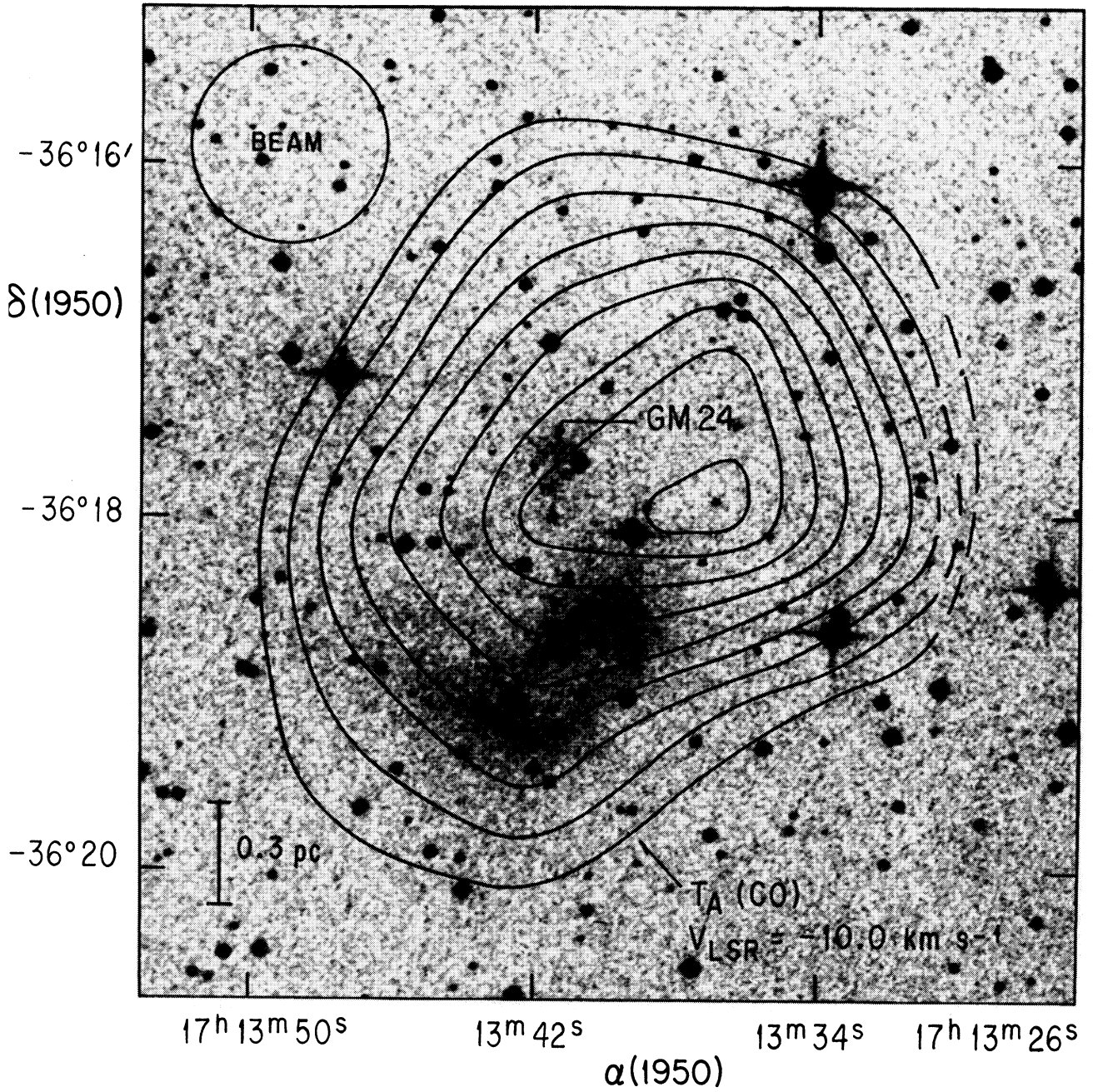
Fig. 7. Contour map of the antenna temperature of the $J = 1 \to 0$ CO transition at $V_{LSR} = -10.0$ km s^{-1} superposed on an optical photograph of the GM 24 region. The lowest contour is 25 K and the increment is 1 K.

J.M. TORRELLES *et al.* (See page 147)